

RADIATION PRESSURE DRIVEN GALACTIC WINDS FROM SELF-GRAVITATING DISKS

DONG ZHANG¹ & TODD A. THOMPSON^{1,2,3}

SUBMITTED TO APJL: MAY 25, 2010

ABSTRACT

We study large-scale winds from self-gravitating disks radiating near the Eddington limit. We show that the ratio of the radiation pressure force to the gravitational force increases with height to a maximum of twice its value at the disk surface. Thus, self-gravitating disks radiating near the Eddington limit are fundamentally unstable to driving large-scale winds. This result stands in stark contrast to the spherically symmetric case, where super-Eddington luminosities are required for wind formation. We apply this theory to galactic winds from starburst galaxies that approach the Eddington limit for dust. For hydrodynamically coupled gas and dust, we find that the asymptotic velocity of the wind is $v_\infty \simeq 2v_{\text{esc}}$, and that $v_\infty \propto \text{SFR}^{0.36}$, where v_{esc} is the escape velocity and SFR is the star formation rate. Both relations are in excellent agreement with observations. We estimate the minimum SFR surface density required for wind formation and the wind mass loss rate \dot{M} in the “single-scattering” limit. The latter implies efficient gas expulsion for low-mass galaxies. We evaluate the effects of both a spherical dark matter halo and an (old) stellar bulge potential. At fixed disk Eddington ratio, both the halo and bulge act to decrease v_∞ and \dot{M} , causing the wind to become bound and form a “fountain flow” with a typical turning timescale of $\sim 0.1 - 1$ Gyr. Thus, bulge formation and halo assembly may halt efficient wind formation, with implications for the growth of galaxies over cosmic time, as well as the metal content of galaxies and the intergalactic medium.

Subject headings: Galaxies: Starburst — Galaxies: Formation — Galaxies: IGM — Galaxies: Halos

1. INTRODUCTION

Galactic-scale winds are ubiquitous in starburst galaxies in both the local and high-redshift universe (Heckman et al. 1990; Heckman et al. 2000; Pettini et al. 2001, 2002; Shapley et al. 2003; Rupke et al. 2005; Sawicki et al. 2008). They are important for determining the chemical evolution of galaxies and the mass-metallicity relation (Dekel & Silk 1986; Tremonti et al. 2004; Erb et al. 2006; Finlator & Davé 2008), and as a primary source of metals in the intergalactic medium (IGM; e.g., Aguirre et al. 2001). Moreover, galactic winds are perhaps the most extreme manifestation of the feedback between star formation in a galaxy and its interstellar medium (ISM). This feedback mechanism is crucial for understanding galaxy formation and evolution over cosmic time (Springel & Hernquist 2003; Oppenheimer & Davé 2006; Oppenheimer & Davé 2008; Oppenheimer et al. 2009).

The most well-developed model for galactic winds from starbursts is the supernova-driven model of Chevalier & Clegg (1985), which assumes that the energy from multiple stellar winds and core-collapse supernovae in the starburst is efficiently thermalized. The resulting hot flow drives gas out of the host, sweeping up the cool ISM (Heckman, Lehnert & Armus 1993; Strickland & Stevens 2000; Strickland et al. 2002; Strickland & Heckman 2009). Although this model is successful in explaining the X-ray properties of starbursts, the recent observational results that galaxies with higher star formation rates (SFRs) accelerate the absorbing cold gas clouds to higher velocities ($v \propto \text{SFR}^{0.35}$) and that the wind velocity is correlated with the galaxy escape velocity challenge the traditional hypothesis that the cool gas is accelerated by the ram pressure of the hot

supernova-heated wind, whose temperature varies little with SFR, circular velocity, and host galaxy mass (e.g., Martin 2005; Weiner et al. 2009). These observations may instead favor momentum-driven or radiation pressure-driven models for the wind physics.

The model that galactic winds may be driven by momentum deposition provided by radiation pressure from the continuum absorption and scattering of starlight on dust grains was developed by Murray, Quataert & Thompson (2005, hereafter MQT05). However, the conclusions of MQT05 are based on an assumed isothermal potential and spherical geometry, and are thus most appropriate for elliptical/spheroidal galaxies. On the other hand, the theory of radiation-driven winds from accretion disks from the stellar to galactic scales has also been studied (e.g., Tajima & Fukue 1996, 1998; Proga, Stone & Drew 1998, 1999; Proga 2000, 2003), but none of these works considered radiation from self-gravitating disks.

In this *Letter* we answer the question of whether or not large-scale winds can be driven by radiation pressure from self-gravitating disks radiating near the Eddington limit. These considerations are motivated by the work of Thompson, Quataert, & Murray (2005), who argued that radiation pressure on dust is the dominant feedback mechanism in starbursts, and that in these systems star formation is Eddington-limited. For simplicity, throughout this paper we assume the disk is of uniform brightness and surface density. In §2, we show that such disks are fundamentally unstable to wind formation because the radiation pressure force dominates gravity in the vertical direction above the disk surface. This result is qualitatively different from the well-known case in spherical symmetry. In §2, we also calculate the terminal velocity of the wind along the disk pole, and its dependence on both the SFR and galaxy escape velocity. In §3, we assess the importance of a spherical stellar bulge and dark matter halo potential. In §4, we discuss the 3-dimensional wind structure and estimate

¹ Department of Astronomy, The Ohio State University, 140 W. 18th Ave., Columbus, OH, 43210; dzhang, thompson@astronomy.ohio-state.edu

² Center for Cosmology & Astro-Particle Physics, The Ohio State University, 191 West Woodruff Ave., Columbus, OH, 43210

³ Alfred P. Sloan Fellow

the total wind mass loss rate. We discuss our findings and conclude in §5.

2. RADIATION-DRIVEN WINDS & THE TERMINAL VELOCITY

We consider a disk with uniform brightness and total surface density: $I(r \leq r_{\text{rad}}) = I$ and $\Sigma(r \leq r_D) = \Sigma$, where r_{rad} and r_D define the outer radius of the luminous and gravitating portion of the disk, respectively. The flux-mean opacity to absorption and scattering of photons is κ . The gravitational force along the polar axis above the disk is

$$\begin{aligned} f_{\text{grav}}(z) &= -2\pi G\Sigma \int_0^{r_D} \frac{zrdr}{(r^2 + z^2)^{3/2}} \\ &= -2\pi G\Sigma \left(1 - \frac{z}{\sqrt{z^2 + r_D^2}} \right), \end{aligned} \quad (1)$$

and the vertical radiation force along the pole (e.g., Proga, Stone & Drew 1998; Tajima & Fukue 1998)

$$f_{\text{rad}}(z) = \frac{2\pi\kappa I}{c} \int_0^{r_{\text{rad}}} \frac{z^2 r dr}{(r^2 + z^2)^2} = \frac{\pi\kappa I}{c} \frac{r_{\text{rad}}^2}{z^2 + r_{\text{rad}}^2}. \quad (2)$$

The Eddington ratio along the pole $\Gamma(z) = |f_{\text{rad}}(z)/f_{\text{grav}}(z)|$ is then

$$\Gamma(z) = \Gamma_0 \left(\frac{r_{\text{rad}}}{r_D} \right)^2 \left(\frac{z^2 + r_D^2}{z^2 + r_{\text{rad}}^2} + \frac{z\sqrt{z^2 + r_D^2}}{z^2 + r_{\text{rad}}^2} \right), \quad (3)$$

where $\Gamma_0 = \Gamma(z=0) = \kappa I / (2cG\Sigma)$ is the Eddington ratio at the disk center. A disk at the Eddington limit ($\Gamma_0 = 1$) requires $I_{\text{Edd}} = 2cG\Sigma/\kappa$, or flux $F_{\text{Edd}} = 2\pi cG\Sigma/\kappa$.⁴ If $r_{\text{rad}}/r_D > 1/\sqrt{2} \simeq 0.7$, then $\Gamma(z)$ increases along the z -axis above the disk. In particular, for $r_{\text{rad}} \simeq r_D$, the radiation force becomes twice the gravitational force as $z \rightarrow \infty$:

$$\Gamma_{\infty} = \Gamma(z \rightarrow \infty) = 2. \quad (4)$$

Because $\Gamma(z)$ increases monotonically with z , the disk is unstable to wind formation. This result for disk geometry is qualitatively different from the spherical case with a central point source where both f_{grav} and f_{rad} are proportional to r^{-2} , and the Eddington ratio is constant.

The velocity of the outflow accelerated along the z -axis by radiation pressure can be written as

$$\frac{v(z)^2 - v_0^2}{4\pi G\Sigma r_D} = \hat{r}\Gamma_0 \arctan\left(\frac{\hat{z}}{\hat{r}}\right) - \left(1 + \hat{z} - \sqrt{1 + \hat{z}^2}\right), \quad (5)$$

where $\hat{r} = r_{\text{rad}}/r_D$, $\hat{z} = z/r_D$, and v_0 is initial vertical velocity. The first term on the right side of equation (5) is the “radiation potential” along the pole, while the second term is the gravitational potential. The limiting value of the total potential at infinity $\hat{r}\Gamma_0 - \pi/2$ is positive if $\hat{r}\Gamma_0 > 2/\pi \simeq 0.64$. Note that in the case of spherical point source, since $v_z^2 - v_0^2 \propto \Gamma - 1$, only super-Eddington objects are able to drive winds. In marked contrast, self-gravitating disks allow the gas above the disk to be accelerated even for some sub-Eddington cases. This is the primary difference between radiation-driven winds from spherical point sources and thin disks.

We introduce the characteristic velocity

$$v_c = \sqrt{4\pi G\Sigma r_D} = 500 \text{ km s}^{-1} \Sigma_0^{1/2} r_{D,1\text{kpc}}^{1/2}, \quad (6)$$

⁴ This is the one-sided disk flux.

where we take $\Sigma_0 = \Sigma/1 \text{ g cm}^{-2} = \Sigma/(4800 M_{\odot} \text{ pc}^{-2})$, and $r_{D,1\text{kpc}} = r_D/1 \text{ kpc}$. From equation (5) with $\Gamma_0 = 1$ and $r_{\text{rad}} \simeq r_D$, the asymptotic terminal velocity along the pole is

$$v_{\infty} = v_c \sqrt{\pi/2 - 1} \simeq 380 \text{ km s}^{-1} \Sigma_0^{1/2} r_{D,1\text{kpc}}^{1/2}. \quad (7)$$

This expression for v_{∞} can be related to the star formation rate (SFR) using the Schmidt law, which relates the star formation surface density and gas surface density in galactic disks: $\Sigma_{\text{SFR}} \propto \Sigma_{\text{gas}}^{1.4}$ (Kennicutt 1998). We approximate $\Sigma_{\text{gas}} = 0.5 f_{g,0.5} \Sigma$, where f_g is the gas fraction. Since $\text{SFR} \sim \Sigma_{\text{SFR}} \pi r_D^2$, we have $v_{\infty} \propto \Sigma^{1/2} r_D^{1/2} \propto \Sigma_{\text{gas}}^{1/2} r_D^{1/2} \propto \text{SFR}^{0.36} r_D^{-0.21}$ or

$$v_{\infty} \sim 400 \text{ km s}^{-1} f_{g,0.5}^{-0.5} \left(\frac{\text{SFR}}{50 M_{\odot} \text{ yr}^{-1}} \right)^{0.36} r_{D,1\text{kpc}}^{-0.21}, \quad (8)$$

which is consistent with the observation $v_{\infty} \propto \text{SFR}^{0.35 \pm 0.06}$ in low-redshift ULIRGs (Martin 2005) and $v_{\infty} \propto \text{SFR}^{0.3}$ for high-stellar-mass and high-SFR galaxies at redshift $z \sim 1$ (Weiner et al. 2009). The scatter at a given SFR may be caused by different r_D , r_{rad}/r_D , v_0 , bulge and dark matter halo mass (see §3). Since we only use a simplified uniform disk model to derive equations (7) and (8), a more definitive comparison with the data should await a model with realistic distributions of surface density, opacity, and brightness.

If we assume the galactic disk is in radial centrifugal balance with a Keplerian velocity $v_{\text{rot}} \sim \sqrt{G\Sigma r}$, and take the mean rotation velocity as half of that at the radius r_D , while the escape velocity is $v_{\text{esc}} \sim \sqrt{2}\langle v_{\text{rot}} \rangle$, equation (7) implies

$$v_{\infty} \simeq 4\sqrt{\pi/2 - 1} \langle v_{\text{rot}} \rangle \simeq 3\langle v_{\text{rot}} \rangle \simeq 2v_{\text{esc}}. \quad (9)$$

This estimate that the terminal velocity of the wind increases linearly with the galactic rotation and escape velocities is also consistent with the observational results in Martin (2005, Fig 7). In their cosmological simulations of structure formation and IGM enrichment by galactic winds, Oppenheimer & Davé (2006) assumed $v_{\infty} = 3\sigma\sqrt{\Gamma_0 - 1} \sim 3\sigma$, where σ is the galactic velocity dispersion (see also Oppenheimer & Davé 2008; Oppenheimer et al. 2009). This factor of 3 is an assumption in their work that is essentially put in by hand. However, our equation (9) shows that it can be derived consistently if the wind is driven by radiation pressure from a self-gravitating disk radiating at or near the Eddington limit. We emphasize that in contrast to the spherical case considered by MQT05, the disk need not be super-Eddington.

Finally, we note that the characteristic timescale for the wind to reach its asymptotic velocity is

$$t_c \sim \sqrt{r_D/(4G\Sigma)} \sim 10^7 \Sigma_0^{-1/2} r_{D,1\text{kpc}}^{1/2} \text{ yr}, \quad (10)$$

which can be compared with the timescale of a bright star-forming disk: $t_{\star} \sim M_{\text{gas}}/\text{SFR}$. Again employing the Schmidt Law, we find that $t_c/t_{\star} \sim 0.03 r_{D,1\text{kpc}}^{1/2} f_{g,0.5}^{1/2} \Sigma_0^{-0.1}$. Therefore, the wind can be accelerated to $\sim v_{\infty}$ before the gas supply is depleted by star formation.⁵

3. BULGE AND DARK MATTER HALO

The galactic bulge and dark matter halo around the galactic disk are important to the wind dynamics. If we do not

⁵ For an instantaneous burst of star formation, the bolometric luminosity decreases on a timescale $t_{\text{MS}} \sim 4 \times 10^6 \text{ yr}$, the main sequence lifetime of the most massive stars. Comparing with equation (10) we see that $t_c \lesssim t_{\text{MS}}$ only when $\Sigma/r \gtrsim 3 \times 10^9 M_{\odot} \text{ kpc}^{-3}$.

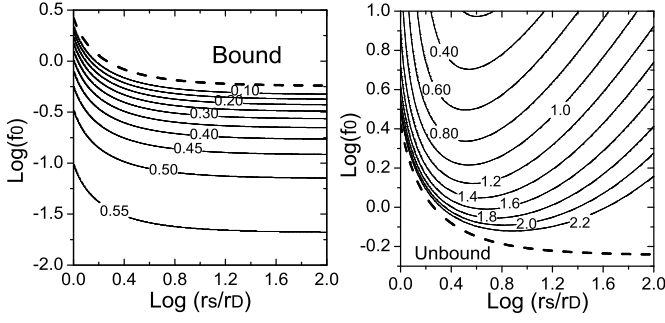


FIG. 1.— Contours of the asymptotic terminal velocity $(v_\infty/v_c)^2$ as a function of $f_0 = f_b + f_h$ (assuming $f_b = 0$) and $c' = r_s/r_D$ for unbound particles (left), and the turning point $\log_{10}(z_{\text{turn}}/r_D)$ along the pole in the case of bound particles, assuming $v_0 = 0$ (right). The dashed line in both panels divides “bound” and “unbound” trajectories.

consider the luminosity from the galactic bulge,⁶ both of the bulge and halo only act to decrease the asymptotic wind velocity, and may even cause the wind to fall back to the disk as a “fountain flow”. The galactic bulge can be taken as a truncated isothermal sphere, and we adopt the NFW potential (Navarro, Frenk & White 1996) to describe the dark matter halo distribution $\rho_{\text{DM}}(r) \propto R^{-1}(R+r_s)^{-3}$, where r_s is the scale radius and $R = \sqrt{r^2 + z^2}$ is the distance to the halo center. For simplicity, in this section we take $r_{\text{rad}} \simeq r_D$. The Eddington limit $\Gamma_0 = 1$ including the dark matter halo becomes

$$\frac{\pi \kappa I}{c} = 2\pi G \Sigma + \frac{1}{2} \frac{GM_{\text{halo}}}{r_s^2 f(c_{\text{vir}})} = 2\pi G \Sigma \left(1 + \frac{f_h}{2c'} \right), \quad (11)$$

where $c_{\text{vir}} = r_{\text{vir}}/r_s$, r_{vir} is the virial radius, $f(c_{\text{vir}}) = \ln(1 + c_{\text{vir}}) - c_{\text{vir}}/(1 + c_{\text{vir}})$, and

$$f_h = \frac{M_{\text{halo}}}{2\pi r_s r_D \Sigma f(c_{\text{vir}})} \sim \frac{M_{\text{halo}}}{M_{\text{disk}}} \left(\frac{r_D}{r_s} \right) \frac{1}{f(c_{\text{vir}})}. \quad (12)$$

We introduce the parameters $c' = r_s/r_D$ and

$$f_b = \frac{1}{2} \left(\frac{M_{\text{bulge}}}{M_{\text{disk}}} \right) \left(\frac{r_D}{r_{\text{bulge}}} \right). \quad (13)$$

The asymptotic velocity of the flow is then (see eq. 5)

$$\frac{v_\infty^2 - v_0^2}{v_c^2} = \Gamma_0 \left(1 + \frac{f_h}{2c'} \right) \frac{\pi}{2} - (1 + f_b + f_h). \quad (14)$$

Note that for $f_b, f_h \rightarrow 0$, equations (14) and (7) are equivalent.

We combine the effects of the galactic bulge and dark matter halo using the parameter $f_0 = f_h + f_b$. Assuming $\Gamma_0 = 1$, the condition for matter to be unbound is

$$f_0 < \left[\left(\frac{v_0}{v_c} \right)^2 + \left(\frac{\pi}{2} - 1 \right) \right] \left(1 - \frac{\pi}{4c'} \right)^{-1} \quad (15)$$

For the typical value $c' \sim 10$, the unbound orbit for a disk with $\Gamma_0 = 1$ requires $f_0 \leq 0.62 + 1.1(v_0/v_c)^2$. If we assume $f_b \ll 1$, and choose the typical value $M_{\text{halo}}/M_{\text{disk}} \sim 10$ and $f(c_{\text{vir}}) \sim 5$, then $f_0 \sim 0.2 < 0.62$, which shows that the matter accelerated by radiation pressure is unbound. In this case, the terminal velocity from equation (14) is less than the value from equation (7), but still satisfies $v_\infty^2 - v_0^2 \sim v_\infty^2 \propto v_c^2$ or $v_\infty \sim \text{SFR}^{0.36}$

⁶ The case of a bright spherical bulge was considered in MQT05.

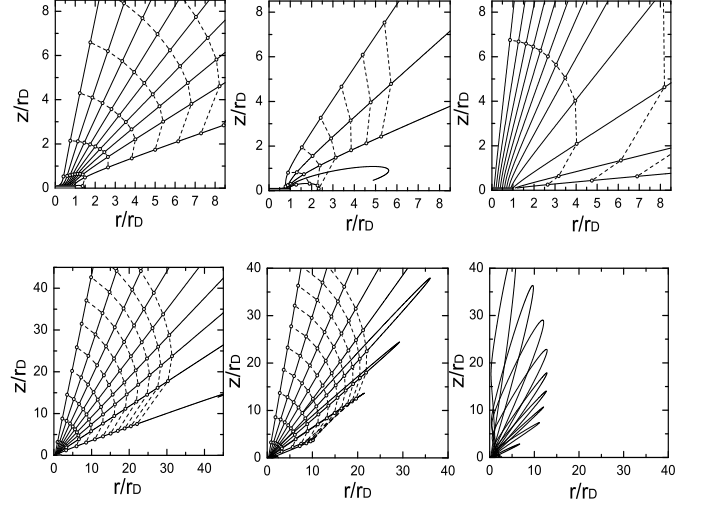


FIG. 2.— The particle orbits from the disk without (upper panels) and with (lower panels) NFW potential. Upper panels, left to right, we take $\Gamma_0 = 1, 0.88$ and 5 . The particle positions and constant time surfaces are labeled at $t/t_c = 2, 4, 6, 8, 10, \dots$, where $t_c = \sqrt{r_D/(4G\Sigma)}$ (eq. 10). Lower panels, left to right: $f_0 = 0.2, 0.6, 1.0$ with $\Gamma_0 = 1$ and $c' = 10$. Constant time surfaces are marked at $t/t_c = 5, 10, 15, 20, 25, \dots$

for a fixed disk size r_D . For a larger bulge or halo at fixed c' , the increase in f_0 may make the outflow bound.

The left panel of Figure 1 gives contours of the asymptotic terminal velocity $(v_\infty/v_c)^2$ as a function of f_0 and c' . The dark matter halo potential well is too deep for particles to escape the disk for large f_0 . In this case, we calculate the “turning point” (z_{turn}) along the pole, which is the maximum height particles reach. The right panel of Figure 1 shows the turning point in the case $v_0 = 0$. A disk with a more massive dark matter halo usually has large f_0 , smaller z_{turn} , and shorter timescale for reaching the turning point $\sim z_{\text{turn}}/v_c$.

4. 3-DIMENSIONAL WINDS AND MASS LOSS RATE

So far we have focused on the forces along the polar z -axis. Figure 2 shows 2-dimensional (2D) projections of the 3D orbits of particles accelerated by radiation pressure and gravity, as well as their constant time surfaces above a uniform disk, starting from an initial height $0.1r_D$, both with and without an NFW potential, and with no galactic bulge. In the absence of a halo, the upper middle panel shows that winds can be driven even when the disk is sub-Eddington ($\Gamma_0 = 0.88$). The lower panels show that a moderately massive halo ($f_0 = 0.6$) prevents matter emerging from the outer disk region from being accelerated to infinity, while a more massive halo with $f_0 = 1$ produces only a “fountain flow” in which particles fall back to the disk with a timescale of $\sim 0.1 - 1$ Gyr. Moreover, Figure 3 gives the vertical velocity v_z evolution of the particles driven from different disk regions. For the face-on disk, the velocity v_z of the wind is just the velocity along the line of sight. The terminal velocities of particles from the outer disk region are smaller than those from the inner disk region. As in Figure 2, matter from the outer region of the disk can be bound by the halo’s gravitational potential even though matter from the inner region is unbound.

To estimate the mass loss rate from Eddington-limited

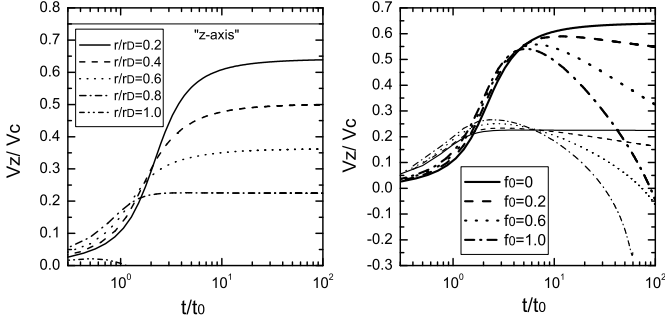


FIG. 3.— *Left panel:* The time evolution of v_z/v_c for $r/r_D = 0.2$ to 1.0 starting with $z/r_D = 0.1$ and $\Gamma_0 = 1$. The horizon line labeled as “z-axis” is the analytic solution of $v_\infty/v_c = \sqrt{\pi/2 - 1}$ as in equation (7). *Right panel:* the velocity v_z/v_c starting from $(r/r_D, z/z_D) = (0.2, 0.1)$ (thick lines) and $(0.8, 0.1)$ (thin lines) with different values f_0 for the dark matter potential with $c' = 10$ and $\Gamma_0 = 1$.

disks, we first note that the flux and luminosity are

$$F_{\text{Edd}} = 2\pi c G \Sigma / \kappa \sim 3 \times 10^{12} \Sigma_0 \kappa_1^{-1} L_\odot \text{ kpc}^{-2}, \quad (16)$$

and

$$L_{\text{Edd}} = \pi r_{\text{rad}}^2 F_{\text{Edd}} \sim 9 \times 10^{12} \left(\frac{r_{\text{rad}}}{r_D} \right)^2 \Sigma_0 \kappa_1^{-1} r_{D, \text{kpc}}^2 L_\odot, \quad (17)$$

respectively, where $\kappa_1 = \kappa / 10 \text{ cm}^2 \text{ g}^{-1}$ is the flux-mean dust opacity. In the single-scattering limit (i.e., all photons from the disk are scattered once in the wind; e.g., MQT05) we estimate the mass loss rate as

$$\dot{M}_W v_\infty \sim L_{\text{Edd}} / c. \quad (18)$$

Combining equations (7) and (18) we have

$$\dot{M}_W \sim 5 \times 10^2 \left(\frac{r_{\text{rad}}}{r_D} \right)^2 \Sigma_0^{1/2} \kappa_1^{-1} r_{D, \text{kpc}}^{3/2} M_\odot \text{ yr}^{-1}, \quad (19)$$

which is consistent with observational results (e.g., Martin 2005, 2006). Note that κ_1 is between the FIR limit $\kappa_{\text{FIR}} \sim 1$ and UV limit $\kappa_{\text{UV}} \sim 10^3 \text{ cm}^2 \text{ g}^{-1}$. The estimate for \dot{M}_W thus varies by 2–3 orders of magnitude from FIR-thick to UV-thin disks. However, using $L = \epsilon c^2 \text{ SFR}$, where $\epsilon_{-3} = \epsilon / 10^{-3}$ is an IMF-dependent constant, the single-scattering estimate for the ratio of the wind mass loss rate to the SFR is

$$\frac{\dot{M}_W}{\text{SFR}} \sim \frac{\epsilon c}{v_\infty} \sim 0.8 \epsilon_{-3} \Sigma_0^{-1/2} r_{D, \text{kpc}}^{-1/2}, \quad (20)$$

which implies that the expulsion of matter by radiation pressure driven winds may be very efficient in low-mass galaxies: for example, $\dot{M}_W / \text{SFR} \gtrsim 10$ for $\Sigma r_D \lesssim 3.1 \times 10^4 M_\odot \text{ pc}^{-1}$.

If we include the dark matter halo or bulge potential, \dot{M}_W decreases. In the unbound case $v_\infty > 0$ equation (18) becomes $\dot{M}_W v_\infty \sim L_{\text{Edd}} / c - 2\dot{M}_W |\Phi| / v_\infty$ where $|\Phi| = |\Phi_\infty - \Phi_0|$ is the total variation of halo potential. For the NFW potential $|\Phi| = 2f_h G \pi \Sigma r_D$, and $\dot{M}_W \sim L_{\text{Edd}} / (c v_\infty) (1 + 2|\Phi| / v_\infty^2)^{-1}$. For $f_h \sim 0.2$, $c' \sim 10$, we find that $\dot{M}_W \sim 4 \times 10^2 \Sigma_0^{1/2} \kappa_1^{-1} r_{D, \text{kpc}}^{3/2} M_\odot \text{ yr}^{-1}$, somewhat smaller than the result in equation (19). However, for larger f_h , so that $v_\infty \rightarrow 0$ or $|\Phi| \gg v_\infty^2$, $\dot{M}_W \sim (L_{\text{Edd}} / c) (v_\infty / 2|\Phi|) \propto v_\infty$, which decreases linearly with the terminal velocity. Similar relations can be expected for a large bulge potential (f_b ; eq. 13).

Finally, we note that because there is a maximum flux-mean dust opacity of $\kappa \sim 10^3 \text{ cm}^2 \text{ g}^{-1}$, that there is a minimum F_{Edd} (see eq. 16), which, in turn implies a minimum critical star formation rate surface density, $\dot{\Sigma}_{*, \text{min}}^{\text{crit}}$, required for winds.

Employing the observed Schmidt law, $\dot{\Sigma}_{*, \text{min}}^{\text{crit}} \sim 0.2 f_{g, 0.5}^{-7/2} M_\odot \text{ yr}^{-1} \text{ kpc}^{-2}$,⁷ suggestively close to the value found by Heckman (2003).

5. CONCLUSIONS & DISCUSSION

In this letter we study the large-scale winds from self-gravitating disks radiating near the Eddington limit. Different from the spherical case, where the Eddington ratio $\Gamma = f_{\text{rad}} / f_{\text{grav}}$ is a constant with distance from the source, for disks Γ increases to a maximum of twice its value at the disk surface. As a result, self-gravitating disks radiating at (or even somewhat below) the Eddington limit are unstable to driving large-scale winds by radiation pressure.

We quantify the characteristics of the resulting outflow in the context of near-Eddington starbursts, motivated by the work of TQM05 who argued that radiation pressure on dust is the dominant feedback process in starburst galaxies. We find that the asymptotic terminal velocity along the polar direction from disks without a stellar bulge or dark matter halo is $v_\infty \sim \sqrt{4\pi G \Sigma r_D} \sim 2v_{\text{esc}}$, where r_D is the disk radius, Σ is the surface density, v_{esc} is the escape velocity (see eqs. 7 and 9), and may range from $\sim 50 - 1000 \text{ km s}^{-1}$ for starbursts, depending on the system considered. Furthermore, by employing the observed Schmidt law, we find that $v_\infty \propto \text{SFR}^{0.36-0.21} r_D^{-0.21}$ (see eq. 8). Our results are in good agreement with recent observations (e.g., Martin 2005, 2006; Weiner et al. 2009). The typical mass loss rate from an Eddington-limited disk in the single-scattering limit is given by equation (19) and suggests these outflows may efficiently remove mass (eq. 20), particularly from very low-mass galaxies. Both wind velocities and mass loss rates can be significantly decreased by the presence of a bulge or dark matter halo potential (§3). Deeper or more extended spherical potentials cause the flow to be bound and produce only “fountain flows” where particles fall back to the disk on a typical timescale of $\sim 0.1 - 1 \text{ Gyr}$ (see Figs. 1-3). The criterion for the flow to become bound is given in equation (15).

Clearly, more detailed work is required to fully assess radiation pressure on dust as the mechanism for launching cool gas from starburst disks. The main limitation of the work presented here is that we consider only disks with constant brightness and surface density. The general case, with realistic disk brightness, surface density, and dust opacity profiles will modify the picture presented here. Such an effort is underway (Zhang & Thompson, in preparation). However, the basic conclusion that self-gravitating disks radiating near the Eddington limit are able to drive large-scale winds should not be fundamentally changed by more elaborate considerations. Indeed, although we have specialized the discussion to starbursts and dust opacity, the instability derived in §2 is of general applicability.

We thank Norman Murray & Eliot Quataert for many stimulating discussions and for a critical reading of the text. This work is supported in part by NASA grant # NNX10AD01G and by an Alfred P. Sloan Fellowship.

⁷ For consistency with Kennicutt (1998), here we take $\epsilon = 4 \times 10^{-4}$.

REFERENCES

- Aguirre, A., Hernquist, L., Schaye, J., Katz, N., Weinberg, D. H., & Gardner, J. 2001, *ApJ*, 561, 521
- Chevalier, R. A., & Clegg, A. W. 1985, *Nature*, 317, 44
- Davé, R., Oppenheimer, B. D., & Sivanandam, S. 2008, *MNRAS*, 391, 110
- Dekel, A., & Silk, J. 1986, *ApJ*, 303, 39
- Erb, D. K., et al. 2006, *ApJ*, 644, 813
- Finlator, K., & Davé, R. 2008, *MNRAS*, 385, 2181
- Heckman, T. M., Armus, L., & Miley, G. K. 1990, *ApJS*, 74, 833
- Heckman, T. M., Lehnert, M. D., & Armus, L. in Shull, J. M., Thronson, H. A. Jr., eds, *The Environment and Evolution of Galaxies* P. 455 (Kluwer, Dordrecht)
- Heckman, T. M., Lehnert, M. D., Strickland, D. K., & Armus, L., 2000, *ApJ*, 129, 493
- Heckman, T. M. 2003, *Revista Mexicana de Astronomia y Astrofisica Conference Series*, 17, 47
- Kennicutt, Jr. R. C. 1998, *ApJ*, 498, 541
- Martin C. L. 2005, *ApJ*, 621, 227
- Martin C. L. 2006, *ApJ*, 647, 222
- Murray, N., Quataert, E., & Thompson, T. A. 2005, *ApJ*, 618, 569 (MQT05)
- Navarro, J. F., Frenk, C. S., & White, S. D. M. 1996, *ApJ*, 462, 563
- Oppenheimer, B. D., & Davé, R. 2006, *MNRAS*, 373, 1265
- Oppenheimer, B. D., & Davé, R. 2008, *MNRAS*, 387, 577
- Oppenheimer, B. D., et al. astro-ph: 0912.0519
- Pettini, M., et al. 2001, *ApJ*, 554, 981
- Pettini, M., et al. 2002, *ApJ*, 569, 96
- Proga, D. 2000, *ApJ*, 538, 684
- Proga, D. 2003, *ApJ*, 585, 406
- Proga, D., Stone, J. M., & Drew, J. E. 1998, *MNRAS*, 295, 595
- Proga, D., Stone, J. M., & Drew, J. E. 1999, *MNRAS*, 310, 476
- Rupke, D. S., Veilleux, S., & Sanders, D. B. 2005, *ApJS*, 160, 115
- Sawicki, M., et al. 2008, *ApJ*, 687, 884
- Shapley, A. E., Steidel, C. C., Pettini, M., & Adelberger, K. L. 2003, *ApJ*, 588, 65
- Springel, V., & Hernquist, L. 2003, *MNRAS*, 339, 312
- Strickland, D. K., & Stevens, I. R. *MNRAS*, 2000, 314, 511
- Strickland, D. K., Heckman, T. M., Weaver, K. A., Hoopes, C. G., & Dahlem, M. 2002, *ApJ*, 568, 689
- Strickland, D. K., & Heckman, T. M. *ApJ*, 2009, 697, 2030
- Tajima, Y., & Fukue, J. 1996, *PASJ*, 48, 529
- Tajima, Y., & Fukue, J. 1998, *PASJ*, 50, 483
- Thompson, T. A., Quataert, E., & Murray, N. 2005, *ApJ*, 630, 167 (TQM05)
- Tremonti, C. A. et al. 2004, *ApJ*, 613, 898
- Weiner, B. J., et al. 2009, *ApJ*, 692, 187